Supporting Information

G4-SLSELEX-Seq-driven discovery of G4-specific targeting L-RNA aptamer with unique structure features

Tian-Ying Wu [a] and Chun Kit Kwok* [ab]

[a]Department of Chemistry and State Key Laboratory of Marine Pollution, City University of Hong Kong, Kowloon Tong, Hong Kong SAR, China

[b]Shenzhen Research Institute of City University of Hong Kong, Shenzhen, China

*To whom correspondence should be addressed. Tel: +852 3442 6858; Fax: +852 3442 0522; Email: ckkwok42@cityu.edu.hk

Materials and Methods

Table S1. Sequences of the oligonucleotides used in this work.

Table S2. Condition of G4-SLSELEX-Seq for *in vitro* selection process.

Table S3. The enriched sequences in 2nd selection round obtained via next generation sequencing.

Table S4. The enriched sequences in 3rd selection round obtained via next generation sequencing.

Table S5. The enriched sequences in 4th selection round obtained via next generation sequencing.

Table S6. The enriched sequences in 5th selection round obtained via next generation sequencing.

Figure S1 Binding of D-Apt.G5 to *c-kit 1* L-dG4.

Figure S2 Binding of D-Apt.G3 to *c-kit 1* L-dG4 in binding buffer with different concentrations of $MgCl_2$.

Figure S3 Thermal difference spectrum (TDS) of D-Apt.G3.

Figure S4 Ligand-enhanced fluorescence assay of D-Apt.G3 with ThT and NMM.

Figure S5 Ligand-enhanced fluorescence assay of mutant D-Apt.G3 with ThT and NMM.

Figure S6 Schematic of reverse transcription stalling (RTS) and SHALiPE probing.

Figure S7 Binding and SHALiPE probing of D-Apt.G3_ext with L-SL1.

Figure S8 Binding of D-Apt.G3 to *c-kit 1* D-dG4 and L-Apt.G3 to *c-kit 1* L-dG4.

Figure S9 Selectivity of L-Apt.G3 to hybrid dG4 and non-G4 structures.

Figure S10 Competitive Binding of L-Apt.G3 and nucleolin to *c-kit 1* D-dG4.

Materials and Methods

Preparation of Oligonucleotides

All oligonucleotides (oligos) utilized in this study were listed in **Table S1**. L-RNA oligos and L-DNA oligos were purchased from Biosyntech Co., Ltd. (Suzhou, China), D-RNA oligos were purchased from Integrated DNA Technologies Inc (USA) and Huzhou Hippo Biotechnology Co., Ltd. (Huzhou, China). D-DNA oligos were purchased from Genewiz Biotechnology Co., Ltd. (Suzhou, China). Oligos powder was dissolved in UltraPure™ distilled water (DNase- and RNase-free) (Invitrogen) and stored at -30 °C for further use.

G4-SLSELEX-Seq

2 μM Mix ssDNA N18 library was denatured with 3 μM reverse primer for SELEX in 20 mM Tris-HCl buffer (pH 7.5) (Invitrogen) containing 4 mM $MgCl_2$ (Thermo Fisher Scientific, USA), 1 mM Dithiothreitol (DTT) (Invitrogen), 150 mM LiCl (Sigma, USA), and 1 mM dNTP Mix (Promega, USA) at 95 °C for 3 min, and reannealed at 35 °C for 10 min. Then the mixture was incubated with 10 U/μL Superscript III reverse transcriptase (Thermo Fisher Scientific, USA) at 50 °C for 50 min to obtain dsDNA library by primer extension and purified using Zymo-Spin IC DNA Columns (Zymo Research, USA). dsDNA library underwent transcription to produce RNAs with HiScribe T7 High Yield RNA Synthesis Kit (NEB, USA) at 37 °C for 3 h, followed with purification through 10% denaturing polyacrylamide gel electrophoresis (PAGE) and Zymo-Spin IC RNA Column (Zymo Research, USA). Before selection process, Streptavidin Magnetic Beads (750 μg) (MCE, USA) were washed successively with 0.05 M NaCl solution (Invitrogen) containing 0.1 M NaOH (Sigma, USA), and 0.1 M NaCl solution, subsequently blocked with 7.5 μg yeast tRNA (Invitrogen) through rotation at 25 °C, 700 rpm, for 30 min. Defined amount of RNA library pool was denatured in 25 mM Tris-HCl (pH 7.5) containing 1 or 5 mM $MgCl_2$ and 150 mM KCl (Fisher) (**Table S2**), then incubated with 250 μg tRNA-blocked dynabeads for negative selection by shaking at 25 °C, 700 rpm, for 1 or 2 h. Bead-bound RNA sequences were separated and discarded, and supernatant was subjected to incubation with 5'-biotin-*c-kit 1* L-dG4 target for positive selection by shaking at 37 °C, 300 rpm, for 30 min. The mixture was then incubated with remaining tRNA-blocked dynabeads by shaking at 25 °C, 700 rpm, for 30 min. Beads with G4-bound RNAs were separated and washed 5 times with 25 mM Tris-HCl (pH 7.5) containing 1 or 5 mM $MgCl_2$ and 150 mM KCl. G4-bound RNAs were eluted from beads twice with elution buffer (25 mM NaOH and 1 mM EDTA; Invitrogen) with both eluates pooled. The collected eluate was pH-

adjusted using 1 M Tris-HCl (pH 7.5) and subsequently purified via RNA column. Selected RNA sequences were converted to cDNA through reverse transcription by reacting with 0.33 μM reverse primer and 10 U/μL Superscript III reverse transcriptase in 20 mM Tris-HCl (pH 7.5) containing 4 mM $MgCl_2$, 1 mM DTT, 150 mM LiCl, and 1 mM dNTP mixture at 50 °C for 15 min. The reaction was halted with 2 M NaOH at 95 °C for 10 min, and then 1 M Tris-HCl (pH 7.5) was introduced for neutralization. The obtained cDNA was purified with RNA column. cDNA was prepared and amplified with 0.5 μM forward and reverse primers and 2x Kapa Master Mix (Roche, Switzerland) in a 40 μL reaction by PCR. Amplification cycle test was carried out with five aliquots at different cycles before large scale amplification. The amplified dsDNAs were purified with DNA column and transcribed to RNAs for next round of selection. 5 selection rounds were performed, and the conditions of each round were presented in **Table S2**. Following 5 rounds of selection, the amplified dsDNAs from 2nd to 5th rounds were further amplified with next generation sequencing (NGS) primers containing different barcodes by PCR respectively, and NGS analysis was conducted by Guangzhou IGE Biotechnology LTD (China).

Electrophoretic Mobility Shift Assay (EMSA)

Aptamer was denatured and annealed in 25 mM Tris-HCl (pH 7.5) with 10 mM $MgCl_2$ and 150 mM KCl through heating at 95 °C for 5 min and cooling to room temperature (RT) for 20 min. 5'FAM-labeled binding target was mixed with aptamer and incubated at 37 °C for 1 h. After that, binding sample was mixed with 8% glycerol and loaded in 10% native PAGE (19:1, acrylamide: bis-acrylamide) for electrophoresis in 25 mM Tris-HCl (pH 7.5) containing 50 mM KOAc (J&K Scientific, China), and 10 mM $MgCl_2$ at 4 °C, 70 mA for 40 min. Gel image was acquired via Amersham™ Typhoon™ biomolecular imager (Cytiva, USA). The signal intensities of bound band (I_{bound}) and unbound band ($I_{unbound}$) in the gel images were measured via ImageJ software. The Fraction Bound was calculated using the equation: Fraction bound = I_{bound} / (I_{bound} + $I_{unbound}$). The binding curves of EMSA gel were fitted and K_d values and Hill coefficient (h) were obtained using GraphPad Prism with the model of "Specific binding with Hill slope". The equation of this model is $Y = B_{max} * X^h / (K_d^h + X^h)$.

For competition binding assay, L-Apt.G3 in 25 mM Tris-HCl buffer (pH 7.5) containing 10 mM $MgCl_2$ and 150 mM KCl, and FAM-*c-kit 1* D-dG4 were denatured and annealed separately through heating at 95 °C for 5 min and cooling to RT for 20 min. L-Apt.G3 in a concentration gradient and 200 nM DHX36 or nucleolin were added to dG4 target, and incubated at 37 °C for 1 h for competition binding. The binding sample was mixed with 8% glycerol and loaded in 6% non-denaturing PAGE (37.5:1, acrylamide: bis-

acrylamide) for electrophoresis in 25 mM Tris-HCl (pH 7.5) containing 50 mM KOAc, and 10 mM $MgCl_2$ at 4 °C, 35 mA for 70 min. Gel image was acquired by Amersham™ Typhoon™ biomolecular imager (Cytiva, USA). The signal intensities of bound band of protein-G4 complex ($I_{pro\text{-}G4}$) and aptamer-G4 complex ($I_{Apt\text{-}G4}$) in the gel images were measured via ImageQuantTL. The Fraction Bound to DHX36/Nucleolin was calculated using the equation: Fraction bound = $I_{pro\text{-}G4}$ / ($I_{pro\text{-}G4}$ + $I_{Apt\text{-}G4}$). The inhibition curves of EMSA gel were fitted and IC_{50} values were obtained using GraphPad Prism with the model of "[Inhibitor] vs. response -- Variable slope (four parameters)". The equation of this model is Y = [Bottom + (Top - Bottom)] / [1 + (IC_{50} / X)^h].

Ligand-Enhanced Fluorescence Assay

Aptamer (500 nM) was annealed in 25 mM Tris-HCl (pH 7.5) containing 10 mM $MgCl_2$ and 150 mM KCl or LiCl through heating at 95 °C for 5 min, then cooling to RT for 20 min. 2 μM ThT (Solarbio Life Science, China) or NMM (Frontier Specialty Chemicals, USA) was added to the prepared aptamers, with subsequent incubation at RT for 30 min. The mixture was then loaded into a 1-cm path length quartz cuvette. Through exciting the samples at λ_{max} 425 nm for ThT or 399 nm for NMM, the emission spectra of ligand-aptamer complex were acquired using HORIBA FluoroMax-4 fluorescence spectrophotometer (Japan).

Circular Dichroism (CD) Spectroscopy

Apt.G3 (5 μM) was annealed in 25 mM Tris-HCl (pH 7.5) containing 10 mM $MgCl_2$ and 150 mM KCl or LiCl through heating at 95 °C for 5 min, then cooling to RT for 20 min. The aptamer solution was then loaded into a 1-cm path length quartz cuvette and the CD spectra were acquired by a Jasco CD J-150 spectrometer over a wavelength range of 220–320 nm with 1 nm intervals.

UV Spectroscopy

D-Apt.G3 was prepared the same as CD experiments. For thermal difference spectra (TDS), UV spectra were acquired by a Cary 100 UV-Vis spectrophotometer in 20 °C and 95 °C at 295 nm. For UV melting assay, UV spectra were acquired at 295 nm, ranging from 20 °C to 95 °C in 0.5 °C steps.

Reverse Transcriptase Stalling Assay

The 10 μL mixture of Apt.G3_ext (500 nM) and 5'-Cy5 reverse primer (500 nM) in 20 mM Tris-HCl (pH 7.5) containing 4 mM $MgCl_2$, 1 mM DTT, 150 mM KCl/LiCl, and 1 mM dNTP Mix, was denatured at 75 °C for 3 min and reannealed at 35 °C for 10 min. For dideoxy sequencing, a 10 μL mixture of Apt.G3_ext (500 nM), 5'-Cy5 reverse primer (500 nM), and 1 mM dideoxynucleotide (ddNTPs) (Roche) was denatured and reannealed in the same 150 mM LiCl buffer and the same conditions used for RTS assay. Reverse transcription was initiated by introducing 100 U of Superscript III reverse transcriptase. The reaction was conducted at 50 °C for 15 min, then quenched with 0.5 μL of 2 M NaOH through heating at 95 °C for 10 min. Finally, sample was mixed with 10 μL of 2X formamide-denaturing loading dye for denaturing at 95 °C for 10 min and analyzed in 8% denaturing PAGE (19:1, acrylamide: bis-acrylamide) for electrophoresis in 1X TBE (Bio-Rad, USA) at RT, 90 W for 80 min. Gel image was collected by Amersham™ Typhoon™ biomolecular imager (Cytiva, USA).

Selective 2'Hydroxyl Acylation analyzed Lithium ion-mediated Primer Extension (SHALiPE)

The 20 μL mixture of Apt.G3_ext (500 nM) and *c-kit 1* L-dG4 or L-SL1 RNA (0, 1, 5, 10 μM) in 25 mM Tris-HCl (pH 7.5) with 150 mM KCl and 10 mM $MgCl_2$ was denatured at 75 °C for 3 min, with subsequent reannealing at 35 °C for 10 min and incubation at 37 °C for 1 h. 1 μL of 2 M NAI was added to mixture and incubated at 37 °C for 5 min to achieve RNA modification. The reaction was quenched with 5 μL of 2 M DTT and purified via RNA column. The acylated RNA was assessed with the same reaction conditions and procedures as above RTS assay.

Table S1. Sequences of the oligonucleotides used in this work.

Name	Sequence (5'-3')
ssDNA low GC N18 library	TTCTAATACGACTCACTATAGGTTACCAGCCTTCACTGC CGATGCT(N18)[a] AGCATCGGCACCACGGTCGGTCACAC
Forward primer for selection	TTCTAATACGACTCACTATAGGTTACCAGCCTTCACTGC
Reverse primer for selection	GTGTGACCGACCGTGGTGC
Biotin-*c-kit 1* L-dG4	Biotin-AGGGAGGGCGCTGGGAGGAGGG (L-DNA bases)
FAM-*c-kit 1* L-dG4	FAM-AGGGAGGGCGCTGGGAGGAGGG (L-DNA bases)
FAM-*c-kit 1* D-dG4	FAM-AGGGAGGGCGCTGGGAGGAGGG
Forward primer for NGS	TCGTCGGCAGCGTCAGATGTGTATAAGAGACAG**XXXX**GG TTACCAGCCTTCACTGC (**XXXX:** barcode)
Reverse primer for NGS	GTCTCGTGGGCTCGGAGATGTGTATAAGAGACAG**XXXX**G TGTGACCGACCGTGGTGC (**XXXX:** barcode)
D-Apt.12-6	CGCCGCCGGGUAUGAGGGAGGAGGGGGCGGCG
D-Apt.G1	CGAUGCUGAGGAGAGGGCGGGCGGAAGCAUCG
D- Apt.G2	CGAUGCUCGCGGGAGGGCGGGAGGAAGCAUCG
D- Apt.G3	CGAUGCUGACGCGGGCGGGAGGGAGAGCAUCG
D- Apt.G4	CGAUGCUGAGGGAGGAGAGGGCGGAAGCAUCG
D- Apt.G5	CGAUGCUGGGCACGAGGGAGGAGGGAGCAUCG
L-Apt.G3	CGAUGCUGACGCGGGCGGGAGGGAGAGCAUCG (L-RNA bases)
D-Apt.G3-M8	CGAUGCUAACGCGGGCGGGAGGGAGAGCAUCG[b]
D-Apt.G3-M11	CGAUGCUGACACGGGCGGGAGGGAGAGCAUCG
D-Apt.G3-M13	CGAUGCUGACGCAGGCGGGAGGGAGAGCAUCG
D-Apt.G3-M14	CGAUGCUGACGCGAGCGGGAGGGAGAGCAUCG
D-Apt.G3-M15	CGAUGCUGACGCGGACGGGAGGGAGAGCAUCG
D-Apt.G3-M17	CGAUGCUGACGCGGGCAGGAGGGAGAGCAUCG
D-Apt.G3-M18	CGAUGCUGACGCGGGCGAGAGGGAGAGCAUCG
D-Apt.G3-M19	CGAUGCUGACGCGGGCGGAAGGGAGAGCAUCG
D-Apt.G3-M21	CGAUGCUGACGCGGGCGGGAAGGAGAGCAUCG
D-Apt.G3-M22	CGAUGCUGACGCGGGCGGGAGAGAGAGCAUCG
D-Apt.G3-M23	CGAUGCUGACGCGGGCGGGAGGAAGAGCAUCG
D-Apt.G3-M25	CGAUGCUGACGCGGGCGGGAGGGAAAGCAUCG
Cy5-Reverse primer	Cy5-GTGTGACCGACCGTGGTGC

for RTS and SHALiPE assay	
D-Apt.G3_ext	GGUUACCAGCCUUCACUGCCGAUGCUGACGCGGGCGGGA GGGAGAGCAUCGGCACCACGGUCGGUCACAC
L-SL1 RNA	GGUUUAUACCUUCCCAGGUAACAAACC (L-RNA bases)
FAM-*c-myc* D-dG4	FAM-GGAGGGTGGGGAGGGTGGGGAA
FAM-c-*kit 2* D-dG4	FAM-CGGGCGGGCGCGAGGGAGGGG
FAM-*Bcl-2mid* D-dG4	FAM-GGGCGCGGGAGGAAGGGGGCGGG
FAM-TBA D-dG4	FAM-GGTTGGTGTGGTTGG
FAM-1I34 D-dG4	FAM-GGTTTTGGCAGGGTTTTGGT
FAM-148D D-dG4	FAM-GGTTGGTGTGGTTGGTT
FAM-*Hras-1* D-dG4	FAM-TCGGGTTGCGGGCGCAGGGCACGGGCG
FAM-*hTelo* D-dG4	FAM-TTAGGGTTAGGGTTAGGGTTAGGG
FAM-SYNDIG1 D-dG4	FAM-GGATGATGTTGGGCCGGTAGCGGG
FAM-AKT1 D-dG4	FAM-GGGCCGTGGGGCTCCCCGGGCGCTGGG
FAM-2GKU D-dG4	FAM-TTGGGTTAGGGTTAGGGTTAGGGA
FAM-*hTERC* D-rG4	FAM-GGGUUGCGGAGGGUGGGCCU
FAM-*KRAS* D-rG4	FAM-GCGGCGGCGGAGGCA
FAM-*bcl-2* D-rG4	FAM-GGGGGCCGUGGGGUGGGAGCUGGGG
FAM-*APP* D-rG4	FAM-GGGGCGGGUGGGGAGGGG
FAM-PolyA D-RNA	FAM-AAAAAAAAAAAAAAAAA
FAM-PolyC D-RNA	FAM-CCCCCCCCCCCCCCCCC
FAM-PolyU D-RNA	FAM-UUUUUUUUUUUUUUUUU
FAM-Hairpin D-DNA	FAM-CAGTACAGATCTGTACTG
FAM-Hairpin D-RNA	FAM-CAGUACAGAUCUGUACUG

a) The A:G:C:T ratio in ssDNA N18 library is 35%:15%:15%:35%. b) The mutated bases are in red font.

Table S2. Condition of G4-SLSELEX-Seq for *in vitro* selection process.

Rounds	**1**	**2**	**3**	**4**	**5**
$MgCl_2$ Conc. (mM)	5	5	5	5	1
D-RNA pool (pmol)	1000	100	75	50	50
Biotin-*c-kit 1* L-dG4 (pmol)	200	20	20	10	3
Negative selection (h)	2	2	2	1	1
Positive selection (min)	30	30	30	30	30
Washing (min)	Pipette mix	Pipette mix	Pipette mix	10	10
Temperature (^oC)	37	37	37	37	37

Table S3. The enriched sequences in 2nd selection round obtained via next generation sequencing.

No.	DNA sequence (5'-3')	Number	Reads (%)
1	CGATGCTGAGGGGAGGGCGGAGCGGAGCATCG	42	0.0071
2	CGATGCTCGGGAGGAGCGAGGAGGCAGCATCG	39	0.0066
3	CGATGCTGGGAGGAGCGGGAGGGCGAGCATCG	38	0.0064
4	CGATGCTCGGAGAGGGAGGGCGGGAAGCATCG	38	0.0064
5	CGATGCTAGGGCGGAGCGGGAGGGCAGCATCG	37	0.0062
6	CGATGCTGGGAGGCGAGGGAGGGCAAGCATCG	35	0.0059
7	CGATGCTGGAGAGGAGAGGGCGGGGAGCATCG	34	0.0057
8	CGATGCTGGAGAGGAGAGGGCGGGAAGCATCG	33	0.0056
9	CGATGCTGCGGAGCGGGAGGGCGGAAGCATCG	33	0.0056
10	CGATGCTAAGGGGGGGGCGGAGCGGAGCATCG	32	0.0054
11	CGATGCTAGGGCGGAGAGGGAGGGCAGCATCG	32	0.0054
12	CGATGCTGGCGAGGGAGGGAGGGCAAGCATCG	32	0.0054
13	CGATGCTGGAGAGGGAGGGCGGGCGAGCATCG	32	0.0054
14	CGATGCTAGGGCGGAGAGGGCGGGCAGCATCG	30	0.0051
15	CGATGCTCAGGAGGGGAAGGGAGGCAGCATCG	30	0.0051
16	CGATGCTGAGGAGCGGGGGGGCGGAAGCATCG	30	0.0051
17	CGATGCTCGGAGCGGGAGGGCGGGAAGCATCG	30	0.0051
18	CGATGCTAGGGGAGAGGCGGAGAGGAGCATCG	30	0.0051
19	CGATGCTGAGGGGCGGGAGGCGAGGAGCATCG	30	0.0051
20	CGATGCTGAGGGGAGGGAGGAGCGGAGCATCG	29	0.0049
21	CGATGCTCGAAGGGGGAGGAGGCAGAGCATCG	29	0.0049
22	CGATGCTGAGGGGAGGGAGGAGAGGAGCATCG	29	0.0049
23	CGATGCTAAGGGGCGGGAGGCGAGGAGCATCG	29	0.0049
24	CGATGCTCGGGAGGAGCGGGCGGGAAGCATCG	29	0.0049
25	CGATGCTGAGGGGCGGGAGGAGCGGAGCATCG	29	0.0049
26	CGATGCTGAGGGGAGGGAGGCGCGGAGCATCG	29	0.0049
27	CGATGCTGGGAGGAGAGGGAGGGCGAGCATCG	29	0.0049
28	CGATGCTAGGGGGGGCGGAGAGGGCAGCATCG	29	0.0049
29	CGATGCTCGGCGAGGGAGGGAGGGAAGCATCG	29	0.0049
30	CGATGCTGGAGAGGAGCGGGCGGGAAGCATCG	29	0.0049
31	CGATGCTCAGGGCGGAGGGGCGGGAAGCATCG	28	0.0047
32	CGATGCTGGCGAGGGAGGGGGGGAAAGCATCG	28	0.0047
33	CGATGCTGGAGAGGGGGAGGGCGGGAGCATCG	28	0.0047
34	CGATGCTAGGGCGGGAGGAGCGGGCAGCATCG	28	0.0047
35	CGATGCTGGAGAGGGAGGGCGGGCAAGCATCG	28	0.0047

36	CGATGCTGAGGGGCGGGGGGAGCGGAGCATCG	28	0.0047
37	**CGATGCTGAGGAGAGGGCGGGCGGAAGCATCG**	28	0.0047
38	CGATGCTAAGGGGCGGGAGGAGCGGAGCATCG	28	0.0047
39	CGATGCTGGGGGGAGAGGGAGGGCAAGCATCG	28	0.0047
40	CGATGCTGAGGGGAGGGCGGAGAGGAGCATCG	27	0.0046
41	CGATGCTGAGGGGAGGGAGGCGAGGAGCATCG	27	0.0046
42	CGATGCTAAGGGGAGGGAGGCGAGGAGCATCG	27	0.0046
43	CGATGCTGGGGAGGAAGAGGGCGGGAGCATCG	27	0.0046
44	CGATGCTGGGCGGGAGGAGAGGGCAAGCATCG	27	0.0046
45	CGATGCTCGGGAGGAGCGCGGAGGCAGCATCG	27	0.0046
46	CGATGCTAAGGGGAGGGCGGAGCGGAGCATCG	27	0.0046
47	CGATGCTAAGGGGAGGGCGGCGAGGAGCATCG	27	0.0046
48	CGATGCTAGAGGGAGGAGAGGGCGGAGCATCG	27	0.0046
49	CGATGCTGGAGCGGGAGGGGGGGCGAGCATCG	27	0.0046
50	CGATGCTAGGGCGGCGAGGGAGGGCAGCATCG	27	0.0046
751	**CGATGCTGACGCGGGCGGGAGGGAGAGCATCG**	16	0.0027
1311	**CGATGCTGAGGGAGGAGAGGGCGGAAGCATCG**	13	0.0022
2085	**CGATGCTGGGCACGAGGGAGGAGGGAGCATCG**	12	0.0020
28248	**CGATGCTCGCGGGAGGGCGGGAGGAAGCATCG**	4	0.0007

a) The top 50 enriched sequences and selected aptamer candidates in 2nd selection round are shown. b) Bolded sequences represent selected aptamer candidates for investigation: No.37 (Apt.G1), No.28248 (Apt.G2), No.751 (Apt.G3), No.1311 (Apt.G4) and No.2085 (Apt.G5).

Table S4. The enriched sequences in 3rd selection round obtained via next generation sequencing.

No.	DNA sequence (5'-3')	Number	Reads (%)
1	CGATGCTCGGGAGGAGCGCGGAGGCAGCATCG	236	0.0296
2	CGATGCTCGGGAGGAGCGAGGAGGCAGCATCG	192	0.0241
3	CGATGCTGCGGAGCGGGAGGGCGGAAGCATCG	157	0.0197
4	CGATGCTGCGGAGAGGGCGGGCGGAAGCATCG	135	0.0169
5	CGATGCTGGGGCGGAGCGGAGGAGAAGCATCG	133	0.0167
6	**CGATGCTGAGGAGAGGGCGGGCGGAAGCATCG**	131	0.0164
7	CGATGCTGAGGGGAGGGCGGAGCGGAGCATCG	128	0.0161
8	CGATGCTGAGGGGAGGGAGGCGCGGAGCATCG	127	0.0159
9	CGATGCTGAGGGGAGGGCGGAGAGGAGCATCG	120	0.0151
10	CGATGCTCACGGGGGAGGAGGCAGCAGCATCG	116	0.0146
11	CGATGCTGAGGAGCGGGAGGGCGGAAGCATCG	112	0.0140
12	CGATGCTCGGCGAGGGAGGGAGGGAAGCATCG	112	0.0140
13	CGATGCTGAGGAGCGGGGGGGCGGAAGCATCG	110	0.0138
14	CGATGCTCAGGAGGGGAAGGGAGGCAGCATCG	110	0.0138
15	CGATGCTGAGGGGAGGGAGGCGAGGAGCATCG	108	0.0135
16	CGATGCTGGGAGGAGAGGGCGGGCAAGCATCG	107	0.0134
17	**CGATGCTCGCGGGAGGGCGGGAGGAAGCATCG**	104	0.0130
18	CGATGCTGCGGAGCGGGGGGGCGGAAGCATCG	104	0.0130
19	CGATGCTGGAGAGGGAGGGCGGGGAAGCATCG	103	0.0129
20	CGATGCTGGAGAGGAGAGGGCGGGAAGCATCG	102	0.0128
21	CGATGCTGCGGAGCGGGCGGGCGGAAGCATCG	101	0.0127
22	CGATGCTCGAAGGGGGAGGAGGCAGAGCATCG	100	0.0125
23	CGATGCTGCGGAGAGGGAGGGCGGAAGCATCG	99	0.0124
24	CGATGCTGGGAGGCGAGGGCGGGCAAGCATCG	97	0.0122
25	CGATGCTGAGGGGAGGGCGGCGAGGAGCATCG	97	0.0122
26	CGATGCTGAGGGGCGGGAGGCGAGGAGCATCG	94	0.0118
27	CGATGCTGAGGAGCGGGCGGGCGGAAGCATCG	94	0.0118
28	CGATGCTAAGGGGAGGGCGGAGCGGAGCATCG	93	0.0117
29	CGATGCTGGAGAGGAGAGGGCGGGGAGCATCG	93	0.0117
30	CGATGCTGGGAGGCGAGGGAGGGCAAGCATCG	92	0.0115
31	CGATGCTGCGGAGAGGGCGGGAGGAAGCATCG	91	0.0114
32	CGATGCTCGGAGCGGGAGGGCGGGAAGCATCG	91	0.0114
33	CGATGCTGCGGAGGGGGAGGGCGGAAGCATCG	90	0.0113
34	CGATGCTCGGCGAGGGGGGGAGGGAAGCATCG	89	0.0112
35	CGATGCTGGAGAGGGAGGGCGGGGGAGCATCG	88	0.0110

36	CGATGCTCAAAGGGGGAGGAGGCCGAGCATCG	88	0.0110
37	CGATGCTCGGGAGGAGCGGGAGGGCAGCATCG	87	0.0109
38	CGATGCTCGGAGAGGGAGGGCGGGAAGCATCG	86	0.0108
39	CGATGCTCGGCGAGGGAGGGGGGGAAGCATCG	86	0.0108
40	CGATGCTGAGGGGAGGGCGGCGCGGAGCATCG	85	0.0107
41	CGATGCTAGGGAGGAGAGGGCGGGCAGCATCG	85	0.0107
42	CGATGCTGGCGAGGGAGGGAGGGCAAGCATCG	85	0.0107
43	CGATGCTGAGGGGCGGGAGGAGCGGAGCATCG	84	0.0105
44	CGATGCTCGCGGGAGGGCGGGCGGAAGCATCG	84	0.0105
45	CGATGCTAGGGCGGGAGGCGAGGGCAGCATCG	83	0.0104
46	CGATGCTAGGCGAGGGGGGGCGGGAAGCATCG	83	0.0104
47	CGATGCTAGGCGAGGGCGGGCGGGAAGCATCG	83	0.0104
48	CGATGCTAAGGGGAGGGAGGCGCGGAGCATCG	82	0.0103
49	CGATGCTCGGAGAGGGCGGGCGGGAAGCATCG	80	0.0100
50	CGATGCTGGGAGGGAGGCGAGGGCAAGCATCG	80	0.0100
187	**CGATGCTGAGGGAGGAGAGGGCGGAAGCATCG**	59	0.0074
202	**CGATGCTGGGCACGAGGGAGGAGGGAGCATCG**	58	0.0073
380	**CGATGCTGACGCGGGCGGGAGGGAGAGCATCG**	49	0.0061

a) The top 50 enriched sequences and selected aptamer candidates in 3rd selection round are shown. b) Bolded sequences represent selected aptamer candidates for investigation: No.6 (Apt.G1), No.17 (Apt.G2), No.380 (Apt.G3), No.187 (Apt.G4) and No.202 (Apt.G5).

Table S5. The enriched sequences in 4th selection round obtained via next generation sequencing.

No.	DNA sequence (5'-3')	Number	Reads (%)
1	CGATGCTCGGGAGGAGCGCGGAGGCAGCATCG	837	0.0857
2	CGATGCTGCGGAGCGGGAGGGCGGAAGCATCG	754	0.0772
3	CGATGCTGCGGAGAGGGCGGGCGGAAGCATCG	666	0.0682
4	**CGATGCTGAGGAGAGGGCGGGCGGAAGCATCG**	614	0.0628
5	CGATGCTGAGGAGCGGGAGGGCGGAAGCATCG	609	0.0623
6	CGATGCTGGGGCGGAGCGGAGGAGAAGCATCG	593	0.0607
7	CGATGCTCGGGAGGAGCGAGGAGGCAGCATCG	553	0.0566
8	CGATGCTGAGGAGCGGGGGGGCGGAAGCATCG	496	0.0508
9	CGATGCTGAGGAGCGGGCGGGCGGAAGCATCG	489	0.0500
10	**CGATGCTCGCGGGAGGGCGGGAGGAAGCATCG**	470	0.0481
11	CGATGCTGCGGAGCGGGGGGGCGGAAGCATCG	470	0.0481
12	CGATGCTGCGGAGCGGGCGGGCGGAAGCATCG	449	0.0460
13	CGATGCTGAGGAGAGGGAGGGCGGAAGCATCG	421	0.0431
14	CGATGCTCGCGGGAGGGCGGGCGGAAGCATCG	385	0.0394
15	CGATGCTGAGGGGAGGGCGGAGCGGAGCATCG	380	0.0389
16	CGATGCTGCGCGGGAGGGCGGGAGGAGCATCG	375	0.0384
17	CGATGCTCACGGGGGAGGAGGCAGCAGCATCG	366	0.0375
18	CGATGCTGCGGAGAGGGCGGGAGGAAGCATCG	358	0.0366
19	CGATGCTCGGCGAGGGAGGGAGGGAAGCATCG	353	0.0361
20	CGATGCTGCGGAGAGGGAGGGCGGAAGCATCG	343	0.0351
21	CGATGCTACGCGGGAGGGCGGGAGGAGCATCG	340	0.0348
22	CGATGCTCGGGCGGGAGGGCGGAGAAGCATCG	320	0.0328
23	CGATGCTAGCGGGAGGCGAGGGCGGAGCATCG	311	0.0318
24	CGATGCTCGGAGAGGGAGGGCGGGAAGCATCG	308	0.0315
25	CGATGCTGAGGGGAGGGAGGCGCGGAGCATCG	305	0.0312
26	CGATGCTGAGGGGAGGGCGGCGAGGAGCATCG	303	0.0310
27	CGATGCTCGCGGGAGGGAGGGCGGAAGCATCG	302	0.0309
28	CGATGCTCGGAGCGGGAGGGCGGGAAGCATCG	294	0.0301
29	CGATGCTCGAGGGCGGGAGGGCGGAAGCATCG	289	0.0296
30	CGATGCTCGGAGAGGGCGGGCGGGAAGCATCG	284	0.0291
31	CGATGCTGAGGGGAGGGAGGCGAGGAGCATCG	278	0.0285
32	CGATGCTGCGGAGCGGGCGGGAGGAAGCATCG	273	0.0279
33	CGATGCTGCGGAGGGGGAGGGCGGAAGCATCG	269	0.0275
34	CGATGCTGAGGAGAGGGCGGGAGGAAGCATCG	268	0.0274
35	CGATGCTGGGGACGAGGGAGGAGGGAGCATCG	263	0.0269

36	CGATGCTAGAGGGAGGCGAGGGCGGAGCATCG	262	0.0268
37	CGATGCTCGCGGGAGGGGGGGCGGAAGCATCG	259	0.0265
38	CGATGCTGGAGAGGGAGGGCGGGGAAGCATCG	257	0.0263
39	CGATGCTAGGGACGAGGGAGGCGGGAGCATCG	255	0.0261
40	CGATGCTCGCGGGCGGGAGGGCGGAAGCATCG	254	0.0260
41	CGATGCTCGCGGGAGGGCGGGAGGCAGCATCG	254	0.0260
42	CGATGCTGAGGGGAGGGCGGCGCGGAGCATCG	251	0.0257
43	CGATGCTGCGAGGGAGGCGGGCGGAAGCATCG	250	0.0256
44	CGATGCTGGAGAGGAGAGGGCGGGAAGCATCG	245	0.0251
45	CGATGCTGAGGGGCGGGAGGCGAGGAGCATCG	244	0.0250
46	CGATGCTGAGGAGGGGGCGGGCGGAAGCATCG	242	0.0248
47	CGATGCTCGAGGGAGGGAGGGCGGAAGCATCG	242	0.0248
48	CGATGCTAGCGGGAGGCGCGGGAGGAGCATCG	240	0.0246
49	CGATGCTGGGAGGCGAGGGCGGGCAAGCATCG	240	0.0246
50	CGATGCTGAGGGGAGGGCGGAGAGGAGCATCG	239	0.0245
101	**CGATGCTGAGGGAGGAGAGGGCGGAAGCATCG**	198	0.0203
109	**CGATGCTGGGCACGAGGGAGGAGGGAGCATCG**	194	0.0199
184	**CGATGCTGACGCGGGCGGGAGGGAGAGCATCG**	167	0.0171

a) The top 50 enriched sequences and selected aptamer candidates in 4th selection round are shown. b) Bolded sequences represent selected aptamer candidates for investigation: No.4 (Apt.G1), No.10 (Apt.G2), No.184 (Apt.G3), No.101 (Apt.G4) and No.109 (Apt.G5).

Table S6. The enriched sequences in 5th selection round obtained via next generation sequencing.

No.	DNA sequence (5'-3')	Number	Reads (%)
1	**CGATGCTGAGGAGAGGGCGGGCGGAAGCATCG**	1521	0.2044
2	CGATGCTGCGGAGAGGGCGGGCGGAAGCATCG	1321	0.1775
3	CGATGCTGAGGAGCGGGAGGGCGGAAGCATCG	1265	0.1700
4	CGATGCTGCGGAGCGGGAGGGCGGAAGCATCG	1192	0.1602
5	CGATGCTGAGGAGAGGGAGGGCGGAAGCATCG	1128	0.1516
6	**CGATGCTCGCGGGAGGGCGGGAGGAAGCATCG**	998	0.1341
7	CGATGCTGCGGAGAGGGCGGGAGGAAGCATCG	947	0.1272
8	CGATGCTGAGGAGCGGGGGGGCGGAAGCATCG	789	0.1060
9	CGATGCTGGGGACGAGGGAGGAGGGAGCATCG	779	0.1047
10	CGATGCTCGCGGGAGGGCGGGCGGAAGCATCG	765	0.1028
11	CGATGCTCGAGGGCGGGAGGGCGGAAGCATCG	757	0.1017
12	CGATGCTGAGGAGCGGGCGGGCGGAAGCATCG	737	0.0990
13	CGATGCTGAGGAGAGGGCGGGAGGAAGCATCG	736	0.0989
14	CGATGCTGGGGACGCGGGAGGAGGGAGCATCG	725	0.0974
15	CGATGCTGCGGAGAGGGAGGGCGGAAGCATCG	689	0.0926
16	CGATGCTAGGGACGAGGGAGGCGGGAGCATCG	656	0.0881
17	CGATGCTCGCGGGAGGGAGGGCGGAAGCATCG	643	0.0864
18	CGATGCTGGGGACGAGGGAGGCGGGAGCATCG	642	0.0863
19	CGATGCTGCGGAGCGGGCGGGCGGAAGCATCG	625	0.0840
20	CGATGCTAGAGGGAGGCGAGGGCGGAGCATCG	621	0.0834
21	CGATGCTACGCGGGAGGGCGGGAGGAGCATCG	615	0.0826
22	CGATGCTGCGAGGGAGGCGGGCGGAAGCATCG	611	0.0821
23	CGATGCTGCGGAGCGGGGGGGCGGAAGCATCG	595	0.0799
24	CGATGCTCGAGGGAGGGAGGGCGGAAGCATCG	585	0.0786
25	CGATGCTGCGCGGGAGGGCGGGAGGAGCATCG	572	0.0769
26	**CGATGCTGACGCGGGCGGGAGGGAGAGCATCG**	559	0.0751
27	CGATGCTGGGCACGCGGGAGGAGGGAGCATCG	551	0.0740
28	CGATGCTCGCGGGAGGGCGGGAGGCAGCATCG	533	0.0716
29	CGATGCTAGCGGGAGGCGAGGGCGGAGCATCG	524	0.0704
30	**CGATGCTGAGGGAGGAGAGGGCGGAAGCATCG**	506	0.0680
31	CGATGCTAGGGACGCGGGAGGAGGGAGCATCG	474	0.0637
32	CGATGCTCGAGGGAGGGAGGGAGGAAGCATCG	473	0.0636
33	CGATGCTGAGGGAGGGCGGGCGGCAAGCATCG	467	0.0627
34	CGATGCTACGAGGGAGGCGGGCGGAAGCATCG	464	0.0623
35	**CGATGCTGGGCACGAGGGAGGAGGGAGCATCG**	462	0.0621

36	CGATGCTGAGGAGCGGGCGGGAGGAAGCATCG	448	0.0602
37	CGATGCTGAGGGAGGCGAGGGCGGAAGCATCG	445	0.0598
38	CGATGCTGCGGGAGGAGAGGGCGGAAGCATCG	445	0.0598
39	CGATGCTCGCGGGCGGGAGGGCGGAAGCATCG	444	0.0597
40	CGATGCTAGAGGGAGGCGCGGGCGGAGCATCG	443	0.0595
41	CGATGCTCGAGGGAGGGCGGGAGGAAGCATCG	443	0.0595
42	CGATGCTCACGGGGGAGGAGGCAGCAGCATCG	437	0.0587
43	CGATGCTGACGAGGGAGGGCGGGAGAGCATCG	434	0.0583
44	CGATGCTCGGCGAGGGAGGGAGGGAAGCATCG	432	0.0580
45	CGATGCTGCGAGGGAGGCGGGAGGAAGCATCG	429	0.0576
46	CGATGCTACGAGGGAGGCGGGAGGAAGCATCG	429	0.0576
47	CGATGCTAGCGGGAGGCGCGGGAGGAGCATCG	429	0.0576
48	CGATGCTGCGGAGCGGGCGGGAGGAAGCATCG	428	0.0575
49	CGATGCTCGAGGGAGGGCGGGAGGCAGCATCG	428	0.0575
50	CGATGCTCGCGGGCGGGAGGGAGGAAGCATCG	428	0.0575

a) The top 50 enriched sequences and selected aptamer candidates in 5th selection round are shown. b) Bolded sequences represent selected aptamer candidates for investigation: No.1 (Apt.G1), No.6 (Apt.G2), No.26 (Apt.G3), No.30 (Apt.G4) and No.35 (Apt.G5). c) The G tracts within the loop are in red font.

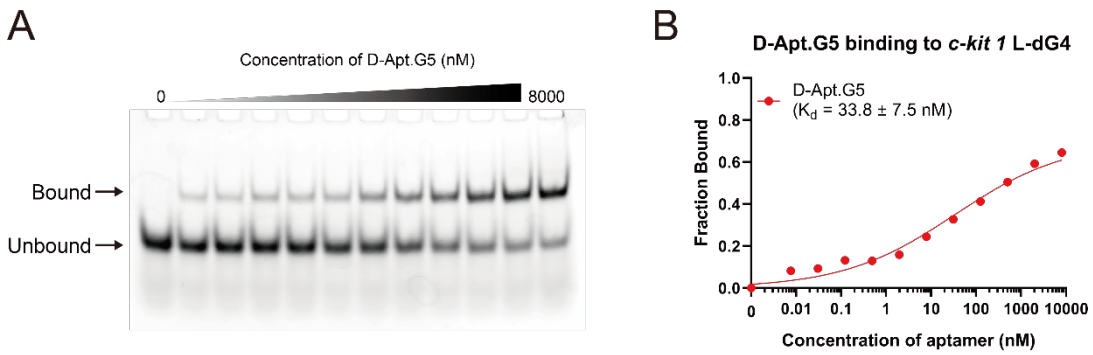

Figure S1 Binding of D-Apt.G5 to *c-kit 1* L-dG4. A) The binding of D-Apt.G5 in a concentration gradient to FAM-*c-kit 1* L-dG4 (10 nM) was assessed using EMSA. The unbound dG4 target shifts upon interaction with D-Apt.G5, and the formation of the bound complex increases as the concentration of D-Apt.G5 rises, indicating the binding of D-Apt.G5 to G4 target. B) The binding curve of D-Apt.G5 to FAM-*c-kit 1* L-dG4 obtained from EMSA gel (A). The dissociation constant (K_d) was found to be 33.8 ± 7.5 nM with Hill coefficient (h) of 0.35, which is around 3-fold higher than that of D-Apt.G3 (**Fig. 2B and 2C**).

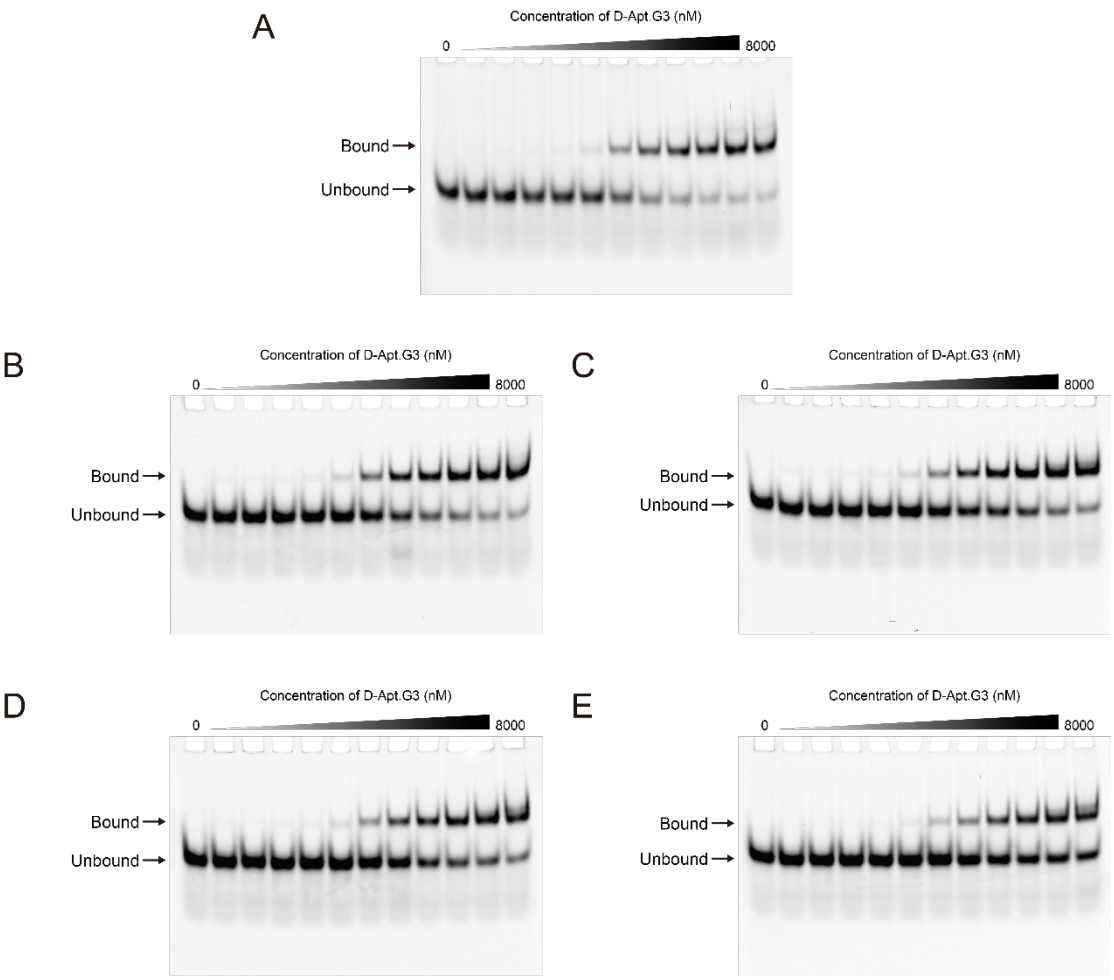

Figure S2 Binding of D-Apt.G3 to *c-kit 1* L-dG4 in binding buffer with different concentrations of $MgCl_2$. The Binding of D-Apt.G3 in a concentration gradient to FAM-*c-kit 1* L-dG4 (10 nM) under buffer conditions with 10 mM $MgCl_2$ (A), 5 mM $MgCl_2$ (B), 2 mM $MgCl_2$ (C), 1 mM $MgCl_2$ (D) and without Mg^{2+} (E) was assessed using EMSA. The binding curves were obtained, and corresponding K_d values were calculated (**Fig. 2E**). With the decrease of Mg^{2+} concentration from 10 mM to 0 mM, the increased unbound target was observed on EMSA gel. Specifically, the K_d of D-Apt.G3 to *c-kit 1* L-dG4 increased from 16.9 ± 1.8 nM to 525.3 ± 120.9 nM, indicating that the binding of D-Apt.G3 to *c-kit 1* L-dG4 is magnesium-dependent, although D-Apt.G3 retains moderate binding capacity in the absence of Mg^{2+}.

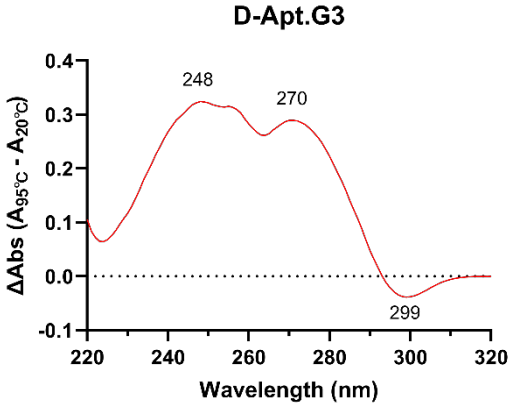

Figure S3 Thermal difference spectrum (TDS) of D-Apt.G3. The UV spectra of D-Apt.G3 at 20 °C and 95 °C were measured at 295 nm. TDS profile of D-Apt.G3 was generated by subtracting the UV absorption at 20 °C from the absorption at 95 °C, which present the UV difference between the folded state and unfolded state of D-Apt.G3. The TDS profile shows positive peaks at 248 nm and 270 nm, along with a negative peak around 299 nm, which are characteristics of a G4 structure. The TDS factor value $\Delta A_{240nm}/\Delta A_{295nm} > 4$ indicates that the G4 in D-Apt.G3 adopts a parallel topology.

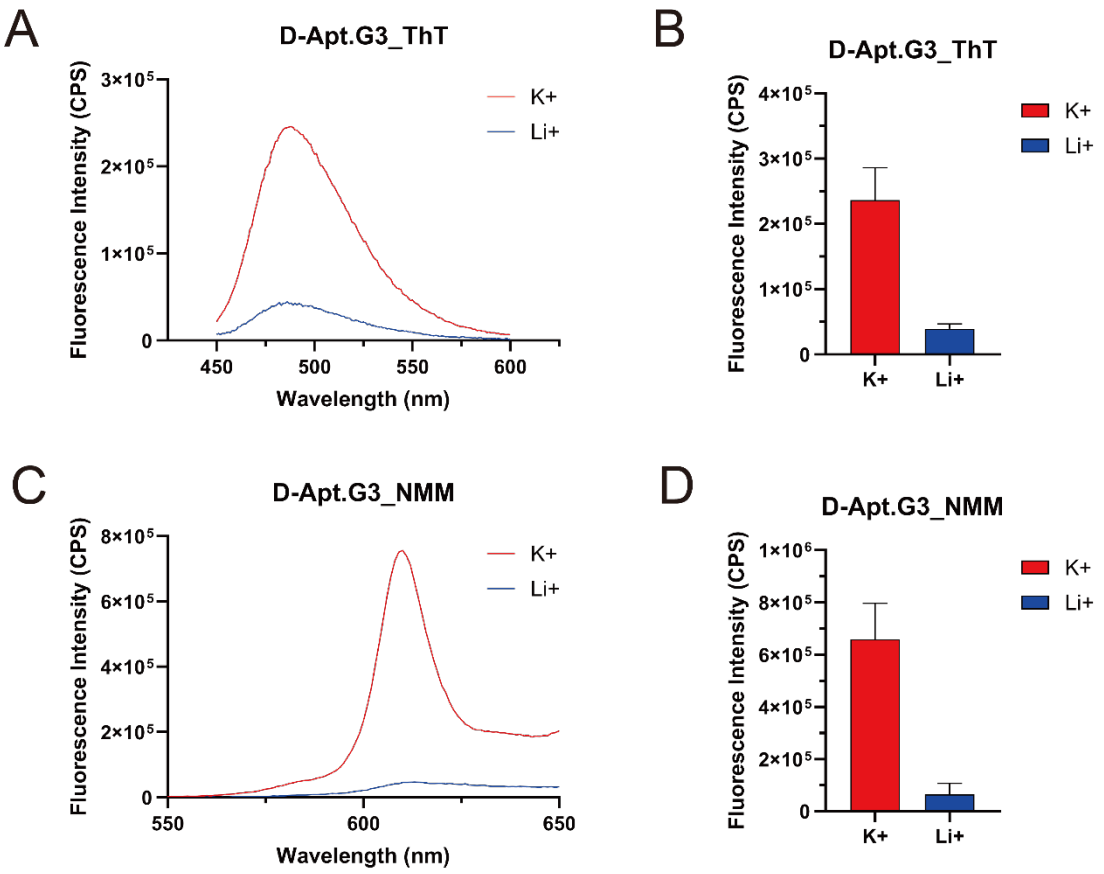

Figure S4 Ligand-enhanced fluorescence assay of D-Apt.G3 with ThT and NMM. Fluorescence emission spectra of ThT (A) and NMM (C) were detected when incubating with D-Apt.G3 under K^+ and Li^+ conditions. The maximum fluorescence emission of ThT and NMM was obtained at 485 nm and 610 nm shown in (B) and (D) respectively. The fluorescence signal of both ThT and NMM enhance significantly when binding to D-Apt.G3 under K^+ conditions with an average 6.1-fold (ThT at λ_{485nm}) and 12.2-fold increase ((NMM at λ_{610nm}). These results confirmed the G4 formation in D-Apt.G3.

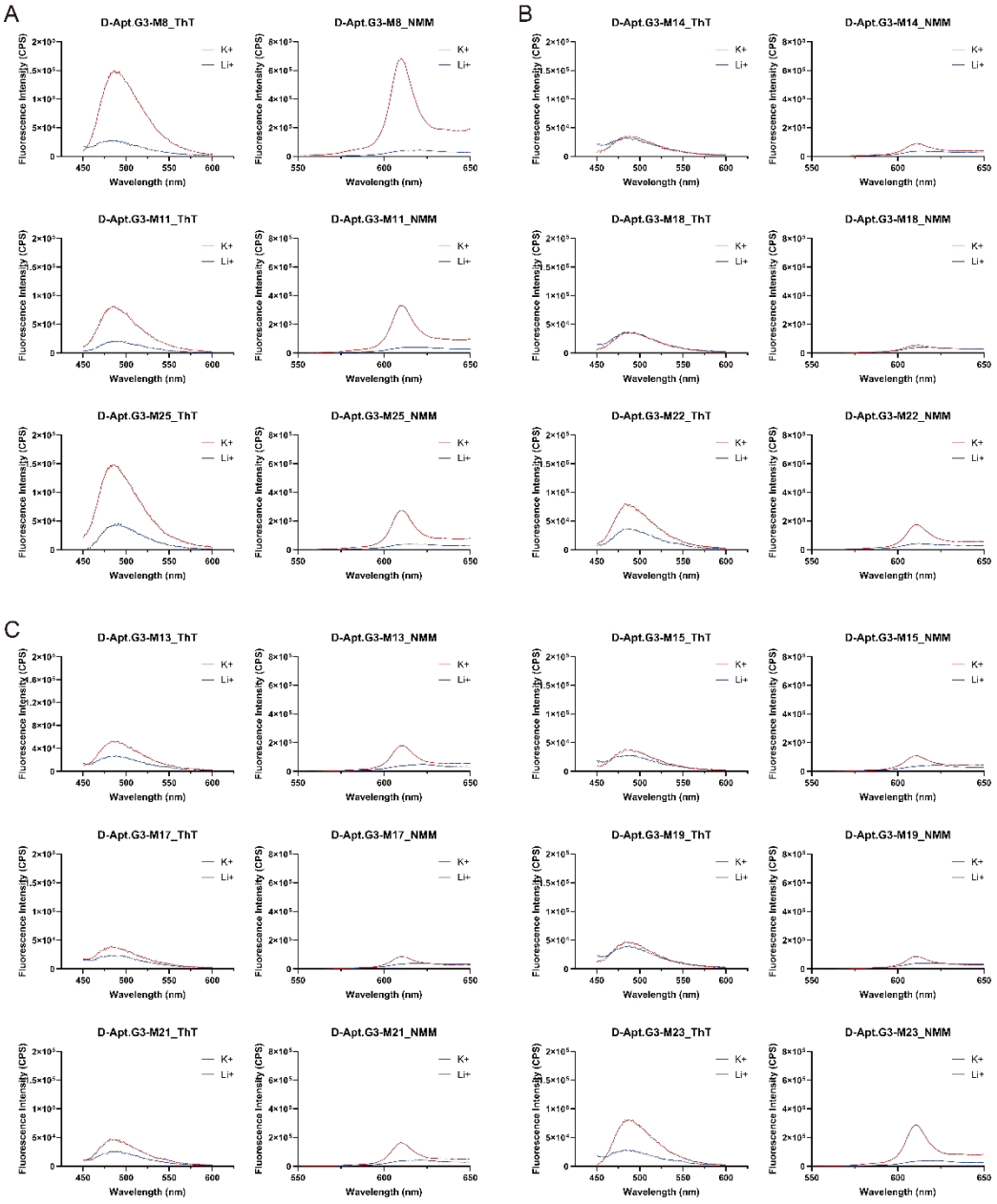
A
D-Apt.G3-M8_ThT
D-Apt.G3-M8_NMM
D-Apt.G3-M11_ThT
D-Apt.G3-M11_NMM
D-Apt.G3-M25_ThT
D-Apt.G3-M25_NMM
B
D-Apt.G3-M14_ThT
D-Apt.G3-M14_NMM
D-Apt.G3-M18_ThT
D-Apt.G3-M18_NMM
D-Apt.G3-M22_ThT
D-Apt.G3-M22_NMM
C
D-Apt.G3-M13_ThT
D-Apt.G3-M13_NMM
D-Apt.G3-M17_ThT
D-Apt.G3-M17_NMM
D-Apt.G3-M21_ThT
D-Apt.G3-M21_NMM
D-Apt.G3-M15_ThT
D-Apt.G3-M15_NMM
D-Apt.G3-M19_ThT
D-Apt.G3-M19_NMM
D-Apt.G3-M23_ThT
D-Apt.G3-M23_NMM
Fluorescence Intensity (CPS)
Wavelength (nm)
K+
Li+

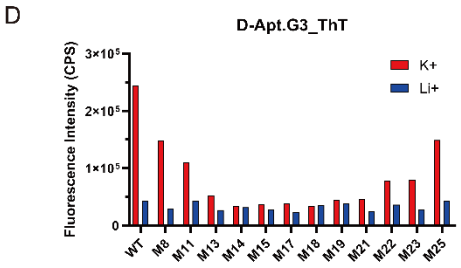
D
D-Apt.G3_ThT
Fluorescence Intensity (CPS)
K+
Li+
WT
M8
M11
M13
M14
M15
M17
M18
M19
M21
M22
M23
M25

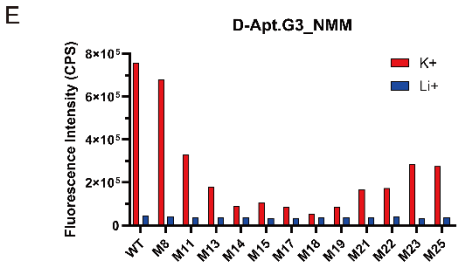
E
D-Apt.G3_NMM
Fluorescence Intensity (CPS)
K+
Li+
WT
M8
M11
M13
M14
M15
M17
M18
M19
M21
M22
M23
M25

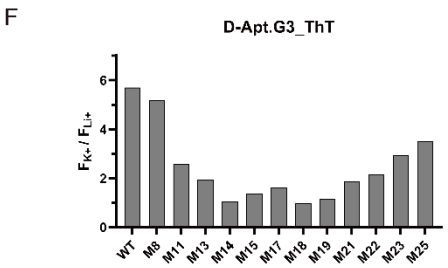
F
D-Apt.G3_ThT
F_K+ / F_Li+
WT
M8
M11
M13
M14
M15
M17
M18
M19
M21
M22
M23
M25

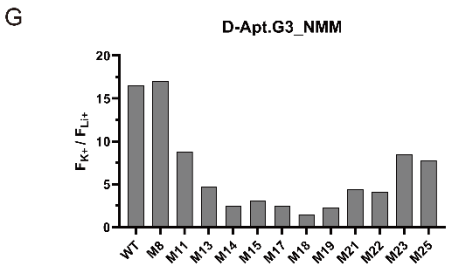
G
D-Apt.G3_NMM
F_K+ / F_Li+
WT
M8
M11
M13
M14
M15
M17
M18
M19
M21
M22
M23
M25

Figure S5 Ligand-enhanced fluorescence assay of mutant D-Apt.G3 with ThT and NMM. The G4 formation of D-Apt.G3 with single mutation of G to A in loop region was assessed under conditions with K^+ and Li^+. Mutations were performed on (A) non-consecutive G residues G8, G11, and G25, (B) the middle Gs in the three consecutive G tracts including G14, G18, and G22, (C) the other G residues in the consecutive G tracts including G13, G15, G17, G19, G22, and G23. The maximum fluorescence emission of ThT and NMM with different D-Apt.G3 mutants were obtained at 485 nm and 610 nm and shown in (D) and (E) respectively. The fold enhancement in fluorescence of ThT (F) and NMM (G) was determined by dividing the fluorescence intensity under K^+ conditions by that under Li^+ conditions. The fluorescence from both ThT and NMM decreased to varying degrees with the addition of different mutants of D-Apt.G3. Additionally, smaller differences in ligand fluorescence between K^+ and Li^+ conditions were observed. Among the tested mutations of D-Apt.G3, substitutions in Gs of the central G tract (G17, G18, and G19) and adjacent two G tracts including G13, G14, G15 and G21, have the greatest effect on G4 formation. Mutations in the remaining G residues in G tracts (G22 and G23) showed intermediate imparts, while non-consecutive Gs (G8, G11, and G25) displayed moderate to negligible effects. These findings suggested that G residues from three consecutive G tracts play critical roles in G4 formation.

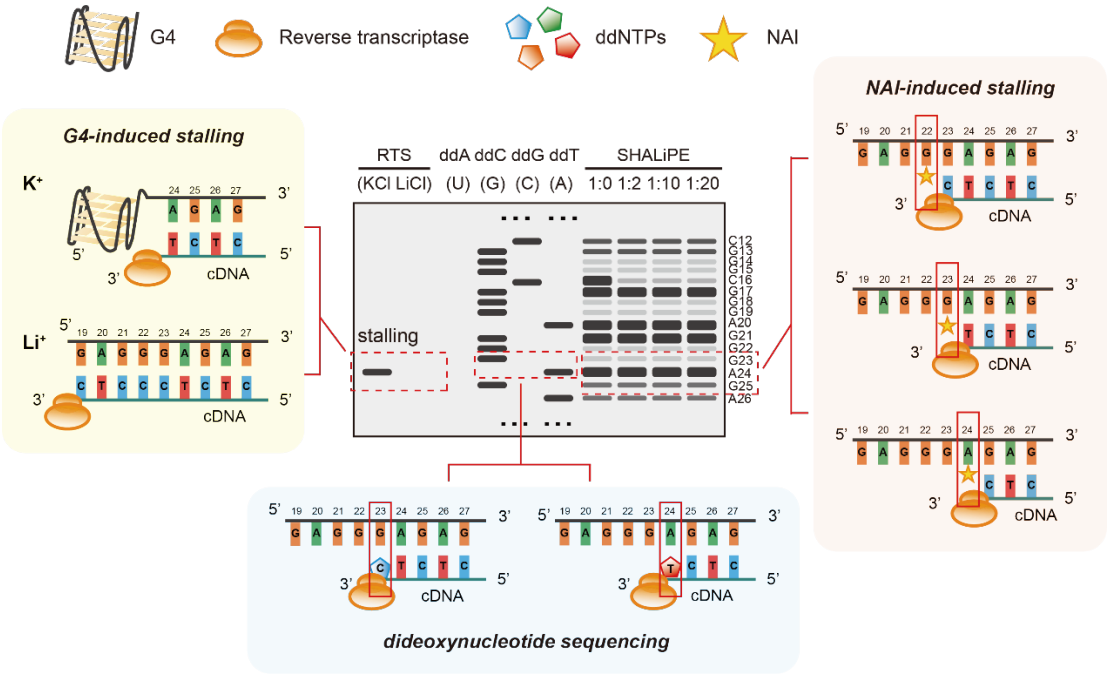

Figure S6 Schematic of reverse transcription stalling (RTS) and SHALiPE probing. In RTS assay, G4 formation in the aptamer (in physiological relevant K^+-containing condition) stalls reverse transcription elongation, producing a stalling band before the G-tracts. On the contrary, G4 is not stabilized in Li^+-containing condition, therefore no stalling band. In dideoxynucleoside (ddNTP) sequencing, each ddNTP incorporation terminates elongation due to the absence of 3'-OH group, generating stalled bands at the position of the incorporated ddNTP. In SHALiPE assay, 2-methylnicotinic acid imidazolide (NAI) modifies the 2'-OH group of flexible nucleotides in single-stranded RNA, stalling reverse transcription and presenting stalled bands located one nucleotide before the modified site.

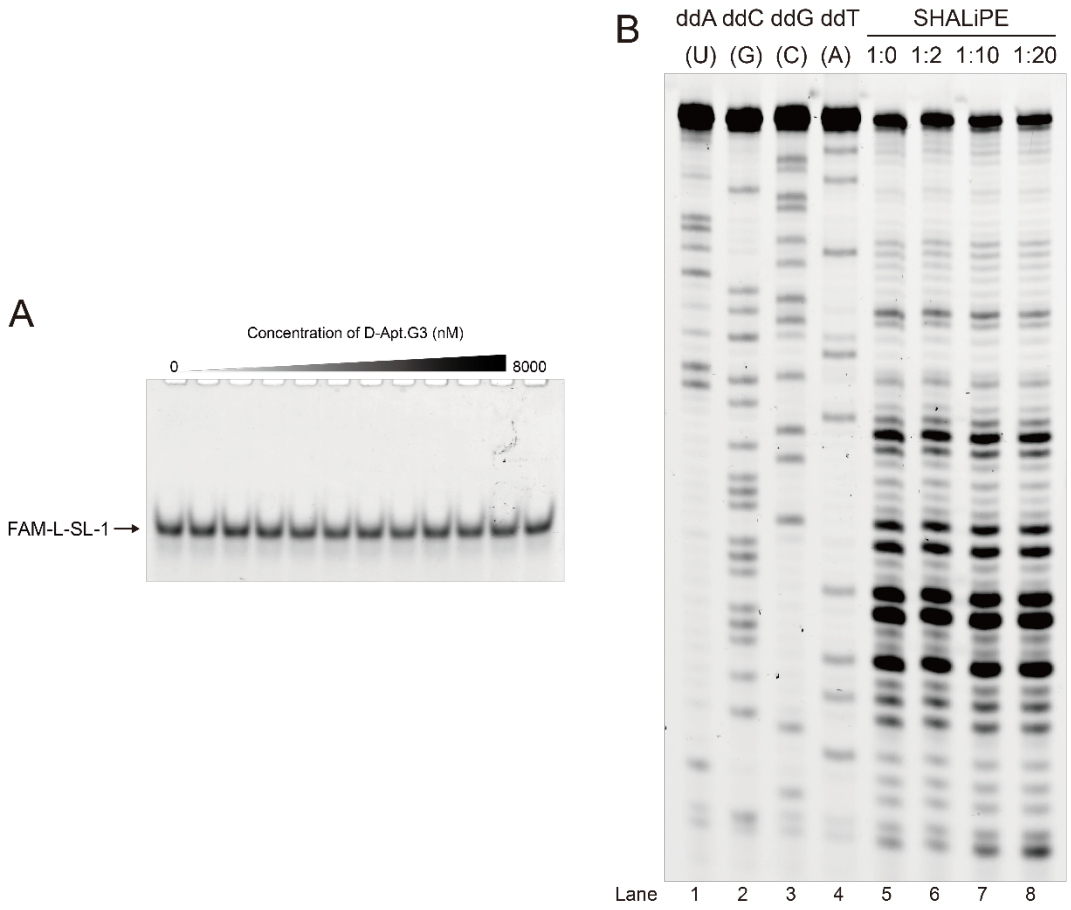

Figure S7 Binding and SHALiPE probing of D-Apt.G3_ext with L-SL1. (A) The binding of D-Apt.G3 in a concentration gradient to FAM-L-SL1 (10 nM) was assessed using EMSA. The result shows no binding between D-Apt.G3_ext with L-SL1, indicating that L-SL1 can work as a negative control for comparison to G4 target in SHALiPE. (B) SHALiPE probing of D-Apt.G3_ext with L-SL1 was assessed. Lanes 1-4: Dideoxy sequencing ladder of D-Apt.G3_ext. Lanes 5-8: SHALiPE probing of D-Apt.G3_ext with increased L-SL1 (1:0, 1:2, 1:10, and 1:20). L-SL1 addition did not affect the NAI reaction with D-Apt.G3_ext, as shown from lane 5 to lane 8.

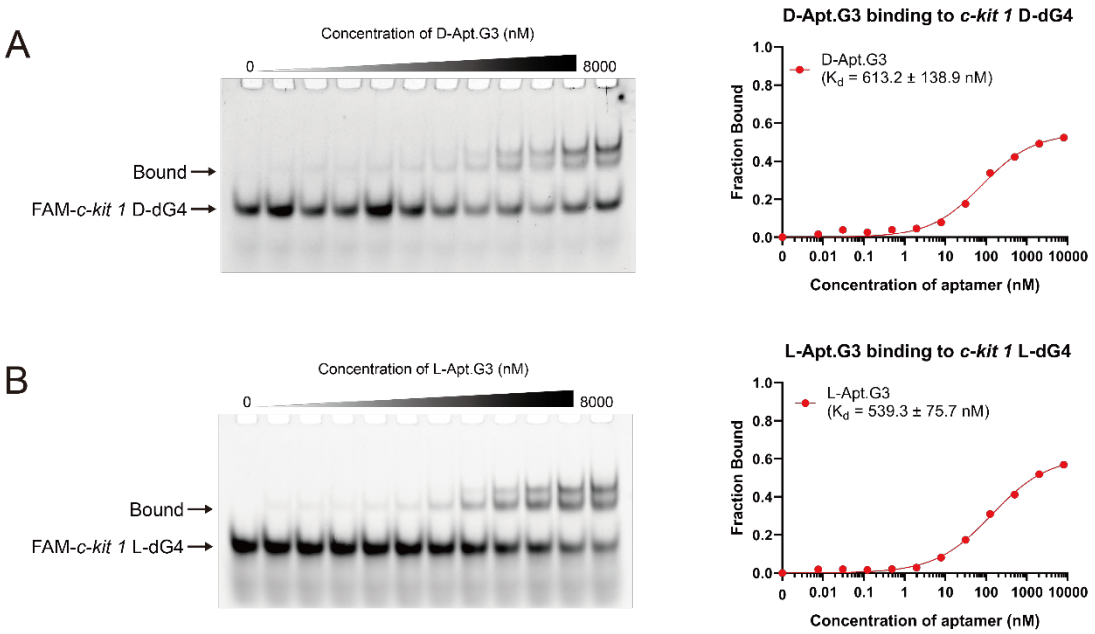

Figure S8 Binding of D-Apt.G3 to *c-kit 1* D-dG4 and L-Apt.G3 to *c-kit 1* L-dG4. A) The binding of D-Apt.G3 in a concentration gradient to FAM-*c-kit 1* D-dG4 (10 nM) was assessed using EMSA and the binding curve was generated from the gel. At high concentrations of D-Apt.G3, multiple bound bands were observed compared to its binding to *c-kit 1* L-dG4 (**Fig. 2B and 2C**). This likely reflects non-specific interactions between D-Apt.G3 and *c-kit 1* D-dG4, resulting in approximately a 51-fold increase in K_d (613.2 ± 138.9 nM, h = 0.38). B) The binding of L-Apt.G3 in a concentration gradient to FAM-*c-kit 1* L-dG4 (10 nM) was assessed using EMSA and the binding curve was generated from the gel. Similar to the binding of D-form aptamers to D-form targets, more than one bound band were observed at high concentrations of L-Apt.G3, compared to its binding to *c-kit 1* D-dG4 (**Fig. 4A and 4B**). This suggests non-specific binding of L-Apt.G3 to *c-kit 1* L-dG4 with a K_d of 539.3 ± 75.7 nM, h = 0.44, which is approximately 61 times greater than the binding of L-form aptamers to D-form target.

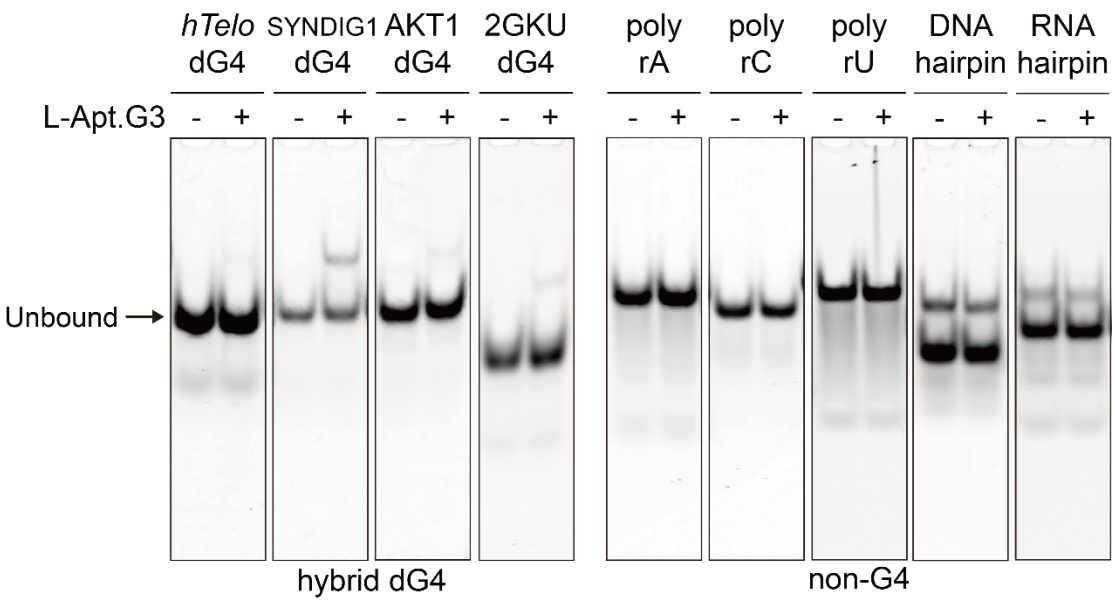

Figure S9 Selectivity of L-Apt.G3 to hybrid dG4s and non-G4 structures. The binding of L-Apt.G3 (50 nM) to 5'FAM-labeled hybrid dG4s including *hTelo* D-dG4, SYNDIG1 D-dG4, AKT1 D-dG4 and 2GKU D-dG4, 5'FAM-labeled non-G4 structures including poly A/C/U D-RNA, D-DNA and D-RNA hairpin were assessed using EMSA. L-Apt.G3 hardly bound to these hybrid dG4s and exhibited no binding to all tested non-G4 structures, suggesting that L-Apt.G3 possesses conformation specificity to parallel and antiparallel G4s rather than hybrid dG4s and non-G4 structures.

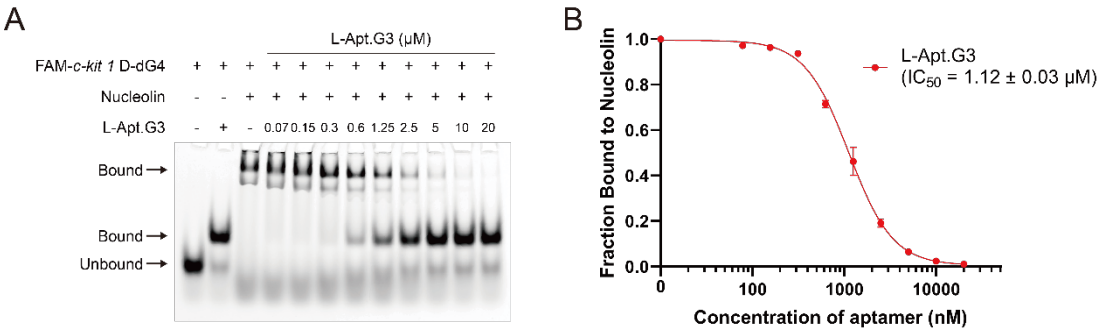

Figure S10 Competitive Binding of L-Apt.G3 and nucleolin to *c-kit 1* D-dG4. A) L-Apt.G3 in a concentration gradient competed with nucleolin (200 nM) to bind FAM-*c-kit 1* D-dG4 (10 nM) assessed by EMSA. Nucleolin strongly bound to *c-kit 1* D-dG4 without aptamer. With the increase of L-Apt.G3, the nuleolin-G4 complex reduced and aptamer-G4 complex increased. B) Inhibition curve of L-Apt.G3 to FAM-*c-kit 1* D-dG4-nuleolin interaction generated from (A). IC_{50} was found to be 1.12 ± 0.03 μM (Error bars: standard deviation, n = 3).